

An Inverted T-shaped MEMS Capacitive Pressure Sensor with Multiple-Diaphragm Anchor and On-chip Temperature Sensor

Yoshihiko Kurui, Fumitaka Ishibashi, Kei Masunishi, Tomohiro Saito, Tomohiko Nagata, Hiroaki Yamazaki and Naofumi Nakamura

Corporate Research & Development Center, Toshiba Corporation, Japan
1, Komukai-Toshiba-cho, Saiwai-ku, Kawasaki-shi, Kanagawa 212-8582, Japan
Phone: +81-44-549-2854 E-mail: yoshihiko.kurui@toshiba.co.jp

Abstract

This paper reports an inverted T-shaped MEMS capacitive pressure sensor with multiple-diaphragm anchor and on-chip temperature sensor for reducing the temperature coefficient. The temperature coefficient can be controlled by changing the number of diaphragms. The on-chip temperature sensor compensates for the temperature characteristics, including the sensor system. The measurement results show that the temperature coefficient was negligibly small at the optimized number. The fabricated pressure sensor system showed a low pressure drift of 0.16% FS at 0–70 °C using temperature compensation.

1. Introduction

Pressure sensors are widely used in industrial, consumer, medical, and automotive applications, among others. Capacitive pressure sensors have advantages such as low power consumption, high sensitivity, and low temperature dependency compared with piezo-resistive sensors [1], as well as disadvantages such as nonlinear output due to non-uniform deformation of the movable electrode. To overcome this problem, MEMS capacitive pressure sensors with an inverted T-shaped electrode have been proposed, in which the movable electrode is separated from the diaphragm using an anchor (Fig.1) [2,3]. The characteristics of the sensor have good linearity compared with conventional sensors because the electrode moves with parallel plate-like displacement that is proportional to the applied pressure. However, the sensor has a temperature drift due to differences in the thermal expansion coefficient of the multi-layered film.

In this paper, we report a MEMS capacitive pressure sensor with multiple-diaphragm anchors (MDAs) and on-chip temperature sensor to drastically reduce the temperature coefficient. Furthermore, we demonstrate low temperature drift and excellent linearity using a capacitive-to-frequency conversion circuit (C-F converter).

2. Design of multiple-diaphragm anchor

Figure 2 shows a schematic of the proposed MEMS pressure sensor with MDAs. The pressure sensor consists of a fixed electrode (Al-Cu), an inverted T-shaped movable electrode (Al), and a diaphragm (amorphous silicon, a-Si). The diaphragm and the movable electrode are connected with MDAs, which are arranged around the center of the movable electrodes. Because the materials of the diaphragm and movable electrode have different thermal expansion

coefficients, the equivalent temperature coefficient of the sensor should be controlled by adjusting the number of diaphragm anchors. To confirm this concept, we fabricated the prototype sensor utilizing a CMOS-compatible surface machining process.

Figure 3 shows a cross-sectional SEM image of a fabricated pressure sensor. The MDAs were successfully fabricated and it was confirmed that this pressure sensor operates at near atmospheric pressure, as shown in the capacitance–pressure curve (Fig. 4). Figure 5 shows the relationship between the number of anchors and the temperature coefficient of the pressure sensor. We confirmed that the temperature coefficient of the pressure sensor varied in the range of negative to positive values by adjusting the number of anchors and demonstrated that the temperature coefficient was negligibly small at the optimized number.

3. Demonstration of a pressure sensor with a C-F converter

To realize a pressure sensor system with high linearity and low temperature drift, we used a readout circuit, as shown in Figure 6(a). The C-F converter was used to detect the capacitance of the pressure sensor. The output frequency of this circuit is inversely proportional to its capacitance value. The frequency has a linear response to applied pressure because of the proportional displacement of the movable electrode.

Because the detection circuit and the post-mounting sensor package have temperature coefficients, the system requires temperature compensation [4]. Therefore, we used an on-chip resistance temperature sensor that was fabricated using the same process as for the pressure sensor and was placed on the same chip. The temperature sensor is composed of an Al–Cu layer having a base resistance of 2.5 K and a sensitivity of 8 Ω /°C. The differential bridge circuit was used to detect the change in resistance of the on-chip temperature sensor because the output voltage is expected to be proportional to the temperature. Figure 6(b) is a prototyped evaluation sensor board. The sensor board consists of a sensor package, readout circuit, and microcomputer. The sensor chip, including the pressure sensor and on-chip temperature sensor, was mounted on a ceramic package with a nozzle.

Figure 7(a) shows the output frequency–pressure curve. We confirmed that the output frequency was proportional to the pressure (2.1% full-scale [FS] nonlinearity) in the range of 700–1500 hPa. The noise floor measured under constant

pressure (1013 hPa) and a conversion time of 40 ms was 2.1 Pa root mean square (rms). Figure 7(b) shows the output voltage–ambient temperature curve. The voltage was acquired from the bridge circuit and on-chip temperature sensor. It showed good linearity (0.35% FS nonlinearity) in the operating range of 0–90 °C and a low noise floor of 0.0018 °C rms.

Figure 8 shows the temperature dependence of the pressure conversion value obtained from the sensor system. The pressure change obtained from the detection circuit (dark dots in Fig. 8) was –123.5 hPa (15.6% FS) in the range of 0–70 °C. The third-degree polynomial fitting was a good match ($R^2 = 0.9999$). However, the pressure change was –1.25 hPa (0.16% FS) due to the introduction of temperature compensation values (red dots in Fig. 8). We succeeded in reducing temperature dependence by 99.0% by introducing temperature compensation.

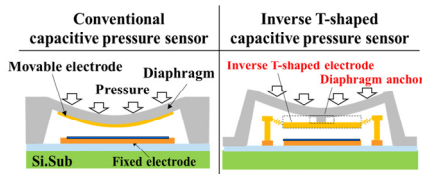


Fig. 1 Features and structures of capacitive pressures

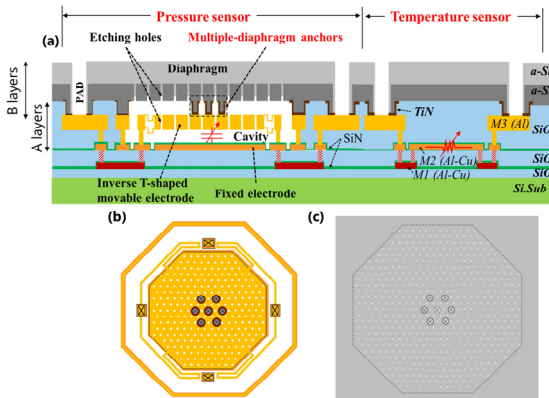


Fig. 2 Schematic of the proposed pressure sensor and on-chip temperature sensor: (a) cross-sectional view; (b) and (c) top view of layers A and B, respectively.

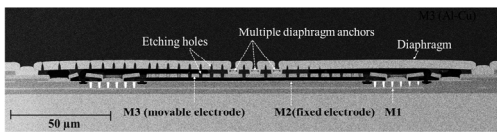


Fig. 3 Optical microscopy images and cross-sectional SEM image of the pressure sensors.

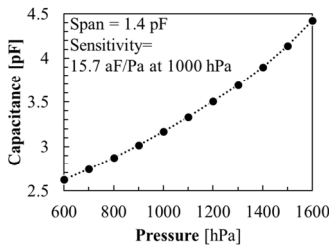


Fig. 4 Measured capacitance as a function of pressure. The sensor has 12 diaphragms, each having a size of 350 μm, connected in parallel.

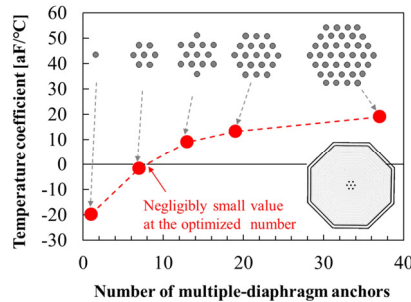


Fig. 5 Measured temperature coefficient as a function of the number of multiple-diaphragm anchors on the pressure sensor with a 200-μm diaphragm

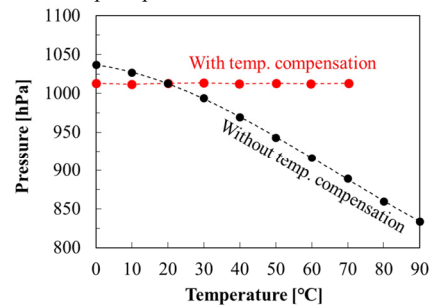


Fig. 8 Measured pressure as a function of temperature on the system, including the sensor package and readout circuit.

4. Conclusion

We proposed an inverted T-shaped MEMS capacitive pressure sensor with a multiple-diaphragm anchor and on-chip temperature sensor. Our sensor showed a drastic reduction in the temperature coefficient following adjustment of the number of diaphragm anchors. Furthermore, we suppressed the temperature characteristics, including in the sensor systems, by using an on-chip temperature sensor (0.16% FS at 0–70 °C).

5 Acknowledgments

This work was supported by the Cabinet Office, Cross-ministerial Strategic Innovation Promotion Program (SIP) “An intelligent knowledge-processing infrastructure, integrating physical and virtual domains” (funding agency: NEDO). Device fabrication of this work was supported by Japan Semiconductor Corporation.

References

- [1] Kirankumar B. Balavalad et al., Sensors & Transducers, Vol. 187, Issue 4, pp. 120-128, 2015.
- [2] D. Ono et al., International Symposium on Micro-Nano Science and Technology, SaA1-B-2, 2016.
- [3] CL Cheng, et al., 2014 IEEE 27th International Conference on Micro Electro Mechanical Systems (MEMS) pp. 757-760, 2014.
- [4] Ville Kaajakari, Practical MEMS: Analysis and Design of Microsystems, 2009.

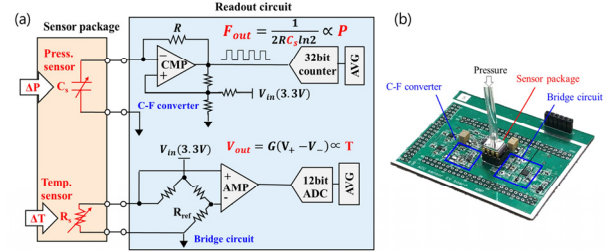


Fig. 6 (a) Block diagram of the pressure sensor system with readout circuit. (b) Evaluation sensor modules.

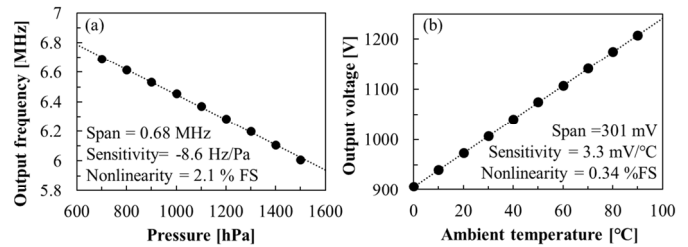


Fig. 7 (a) Measured output of the frequency sensor as a function of pressure on the pressure sensor. The sensor has 12 diaphragms, each having a size of 350 μm, connected in parallel. (b) Measured output voltage as a function of ambient temperature on the on-chip temperature sensor.